Technological University Dublin
ARROW@TU Dublin

Articles | School of Science and Computing

2018

Conformational studies of Gram-negative bacterial quorum sensing acyl homoserine lactone (AHL) molecules: The importance of the n → π* interaction

Goar Sánchez-Sanz

Darren Crowe

Alan Nicholson

See next page for additional authors

Follow this and additional works at: https://arrow.tudublin.ie/ittsciart

 Part of the Chemistry Commons

This Article is brought to you for free and open access by the School of Science and Computing at ARROW@TU Dublin. It has been accepted for inclusion in Articles by an authorized administrator of ARROW@TU Dublin. For more information, please contact arrow.admin@tudublin.ie, aisling.coyne@tudublin.ie, gerard.connolly@tudublin.ie.

This work is licensed under a Creative Commons Attribution-Noncommercial-Share Alike 4.0 License

Authors

Goar Sánchez-Sanz, Darren Crowe, Alan Nicholson, Adrienne Fleming, Ed Carey, and Fintan Kelleher

Biophysical Chemistry 238 (2018) 16–21

Contents lists available at ScienceDirect

Biophysical Chemistry

journal homepage: www.elsevier.com/locate/biophyschem

Conformational studies of Gram-negative bacterial quorum sensing acyl homoserine lactone (AHL) molecules: The importance of the n → π* interaction

Goar Sánchez-Sanz[a], Darren Crowe[b], Alan Nicholson[b], Adrienne Fleming[b], Ed Carey[b], Fintan Kelleher[b,*]

[a] Irish Centre of High-End Computing, Grand Canal Quay, Dublin 2, Ireland
[b] Molecular Design and Synthesis Group, Centre of Applied Science for Health, Institute of Technology Tallaght, Dublin 24, Ireland

HIGHLIGHTS

- AHLs show intermolecular hydrogen-bond in $CDCl_3$ solution.
- DFT calculations of extended and n → π* interaction conformations of AHLs in the gas phase.
- DFT calculations of extended and n → π* interaction conformations of AHLs in the solvent models.
- The n → π* interaction becomes more important with increased dielectric constant of the solvent.

GRAPHICAL ABSTRACT

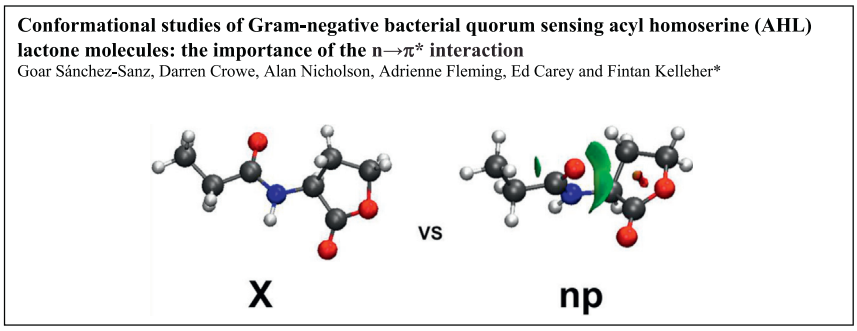

ARTICLE INFO

Keywords:
Acyl homoserine lactones
Quorum sensing
n → π* interaction
DFT calculations
Non-covalent interactions, solvent effects

ABSTRACT

A ^{1}H NMR study shows the presence of intermolecular hydrogen bonds for AHLs in $CDCl_3$ solution. A detailed computational study of the structure of AHLs and the relative stability between the extended conformations (**X**) and those showing n → π* interactions (**np**) have been carried out by means of DFT calculations. Solvent effects have been shown to be very important when stabilising **np** conformations, particularly with polar solvents. This was shown by the shortening of C···O intramolecular distances and the increase in the relative energies favouring the **np** conformation with the dielectric constant of the solvent. The charge transfer between the O donor and the acceptor carbonyl group, assessed by second order perturbation energies, E(2), also shows an increase in the E(2) values with the dielectric constant of the solvent.

1. Introduction

According to the World Health Organisation, Antimicrobial Resistance (AMR) is one of the biggest Global challenges facing mankind [1]. Bacteria which are resistant to all currently used antibiotics are appearing so the requirement for the discovery of new antibiotic classes and compounds has never been more important. Of particular concern is the rise in AMR of Gram-negative species such as *Klebsiella pneumonia*, *Pseudomonas aeruginosa* and *Eschericia coli*, since many of the current antibiotics in development only target Gram-positive species. Bacteria in general have the ability to communicate with each other using molecular signals and when the bacteria reach a threshold

* Corresponding author at: Department of Science, Institute of Technology Tallaght, Tallaght, Dublin 24, Ireland.
E-mail address: fintan.kelleher@ittdublin.ie (F. Kelleher).

https://doi.org/10.1016/j.bpc.2018.04.002
Received 8 March 2018; Received in revised form 10 April 2018; Accepted 10 April 2018
Available online 17 April 2018
0301-4622/ © 2018 Elsevier B.V. All rights reserved.

concentration (quorum) their behaviour can change to that of a multi-celled organism from being single-celled. This ability to detect the numbers of other bacteria in their environment is known as quorum sensing (QS) [2]. Alterations in gene expression ultimately lead to an increase in virulence factors of the bacteria, and one outcome can be the generation of biofilms, which can be highly resistant to antibiotics as the biofilm behaves as a physical barrier to antibiotics. In a number of Gram-negative species the communication molecules secreted are acyl homoserine lactones (AHLs), along with their 3-oxo analogues (OHLs) [3]. Significant effort has gone in to trying to develop analogues of these molecules to inhibit the communication process thus switching off the QS process. Importantly, inhibitors of QS would be bacteriostatic in nature rather than bactericidal, which would mean that there would be less likelihood for the development of resistance [4]. Both AHLs and OHLs contain a γ-lactone head group which is attached, by an amide linker, to an alkyl chain, usually of four to fourteen carbons in length. Therefore, in order design new QS inhibitors a greater understanding of the overall structures and properties of AHLs and OHLs is important.

We recently reported on conformational studies of OHLs by NMR and computational methods [5]. Significantly it was found that there are a number of possible low energy conformations depending on whether the OHLs were studied in the gas phase or in solvent models (computational), in solution (NMR), in the solid state (x-ray crystallography) or bound to their cognate receptor (x-ray crystallography). The 3-oxo group of the side-chain was found to form a hydrogen-bond (HB) with the amide N—H, stabilising a compact conformation. We were next interested in studying in detail the relative stabilities of the AHLs, which lack the 3-oxo group, in terms of their possible conformations.

2. Experimental

The C8 AHL was purchased from Sigma-Aldrich (Irl) Ltd. NMR spectra were obtained in $CDCl_3$, at 25 °C, on a Bruker Avance III 500 spectrometer operating at 500 MHz for ^{1}H NMR. The typical resolution of this machine is 0.11 Hz or 0.00022 ppm. Solutions of the C8 AHL were prepared to a final concentration of 1, 2.5, 5 and 10 mM, and were allowed to equilibrate at ambient temperature, for 7 days before measurement of the spectra.

All systems were optimised using the Gaussian16 package at the M06–2 × [6] computational level with the 6–311 + G(2d,p) basis set. [7] The M06–2 × functional has been shown to properly describe weak interactions, taking into account dispersion forces where other traditional functionals fail. Effects of water solvation have been included, by means of the SCFR–PCM approaches implemented in the Gaussian16 package, including dispersing, repulsing, and cavitating energy terms of the solvent, by starting from the gas–phase geometries and then re-optimising. The electron density of the complexes has been analysed within the Atoms in Molecules (AIM) [8] theory using AIMAll software [9]. The Natural Bond Orbital (NBO) [10] method has been used to analyse the interaction of the occupied and unoccupied orbitals with the NBO–3 program [11] since this kind of interaction is of utmost importance in any charge transfer. The Non-Covalent Interactions (NCI) index, based on the reduced gradient of the electron density, has been calculated to identify attractive and repulsive interactions with the NCI program [12] and plotted with the VMD program [13]

Cartesian coordinates and molecular graphs of all compounds studied at the M06-2x/6–311 + G(2d,p) computational level in the gas phase and PCM solvent models can be found in the electronic supporting information.

3. Results and discussion

3.1. NMR study

NMR solution studies were useful in showing the presence of an intramolecular HB between the 3-oxo carbonyl group and the amide N—H in the OHLs, which would be absent in the AHLs [5]. This absence of a HB leads to a general upfield move in the chemical shift of amide N—H in the AHLs when compared to the OHLs. Since the AHLs contain a number of HB acceptors it was of interest to see whether intermolecular HBs between the amide N—H and any of the HB acceptors are present in solution. Fig. 1 shows a stack of the amide N—H chemical shift of the AHL with a C8 side-chain, as the concentration was increased from 1 mM to 10 mM. The corresponding chemical shifts measured were 5.899 ppm, 5.905 ppm, 5.911 ppm and 5.925 ppm, respectively. Although the overall change in chemical shift is only 0.026 ppm downfield, nonetheless, it is a measurable change, which

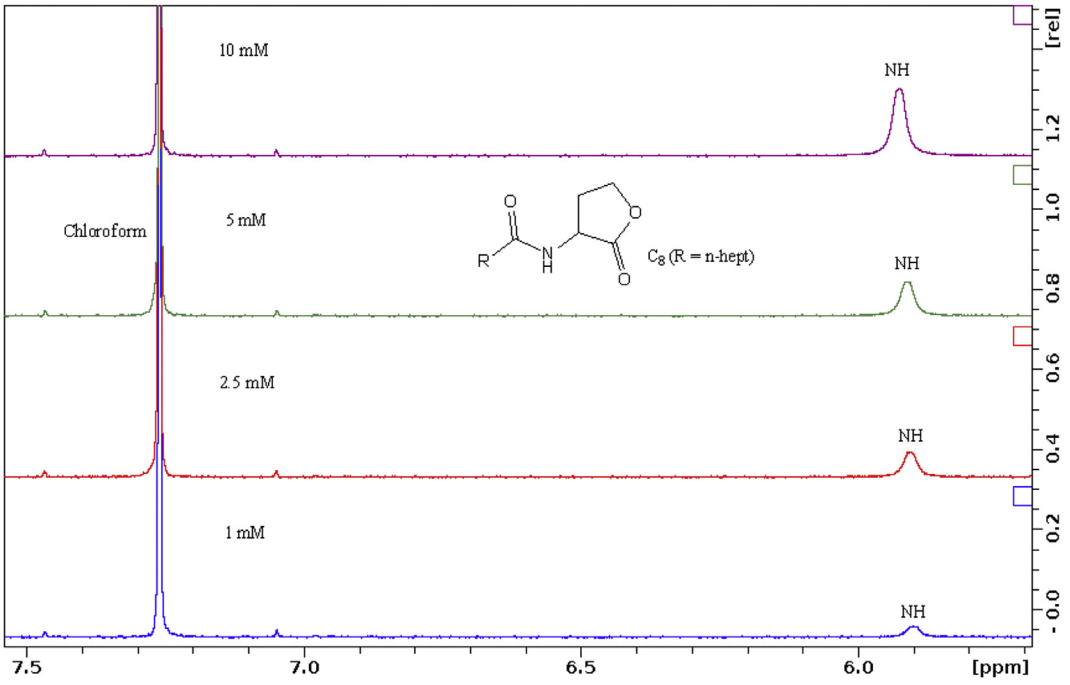

Fig. 1. Stacked ^{1}H NMR spectra of C_8 AHL at 1–10 mM, in $CDCl_3$ at 7 days.

was not observed for the OHLs studied previously, where no changes in chemical shift were observed because of the presence of the intramolecular HBs in $CDCl_3$. For the corresponding C8 OHL the chemical shifts measured were 7.641 ppm, 7.642 ppm, 7.643 ppm and 7.644 ppm, respectively.[5] In this case the overall chemical shift change was only 0.003 ppm. It is not possible to say categorically that there are intermolecular HBs present in AHL solutions in $CDCl_3$, as the changes in chemical shift are so small. At the concentrations used (1–10 mM) it is highly likely that the AHLs are, in fact, monomeric.[5]

3.2. Energy and structure

Computational studies were undertaken, firstly in the gas phase to examine the relative energy differences of possible low energy conformations. From previous results for the analogous OHL molecules it is apparent that non-covalent interactions such as HBs and n → π* are important [5,14–16]. In many literature reports the traditional B3LYP functional is commonly used for DFT calculations. However, where dispersion forces and weak interactions are important, such as n → π* interactions, then it is prudent to test other functionals, such as B3LYP-D3 (with empirical Grimm's dispersion) 17–19. M06-2x [6] and wB97XD [20], which account for long range interactions and can improve the accuracy of the calculations. Furthermore, MP2 calculations [21] were carried out to evaluate the performance of those functionals. MP2 ab initio calculations provide reliable structures and relative energies but they are computationally very demanding and unaffordable for larger systems. Comparing DFT functionals with MP2 will help to benchmark the former and allow for the selection of the most appropriate functional. Initially a series of seven AHL structures were examined (compounds **1**–**7**) to study the effect of the alkyl chain length, branching within the chain (compounds **1**–**6**) and conjugation of the amide carbonyl with a phenyl group (compound **7**). It was found that two different low energy conformations were possible, similar to those found previously for the OHLs (Fig. 2) [5]. The first is an extended structure with the amide N—H and lactone C═O groups being almost *syn*-parallel, denoted **X**, while the second conformation was stabilised by an n → π* interaction and is denoted as **np**.

It can be seen from the results in Table 1, for compounds **1**–**7**, that the relative energy between the conformations **X** and **np**, calculated in the gas phase, do not show large variations across the different functionals used. In all cases it was found that the extended conformation **X** was the more stable. For the DFT calculations the largest variations were found for M06-2x with respect to the B3LYP results; however, all of the results are within the same range. As was mentioned previously, ab initio MP2/6-311 + G(2d,p) calculations were carried out in order to compare the relative energies between **X** and **np** conformations with those values obtained from DFT calculations. In all cases the calculated MP2 relative energy differences for the two conformations are smaller than those provided by any of the DFT calculations. It can be seen that M06-2x functional presents the closest relative energy difference values to the corresponding MP2 ones. In fact, the average relative energy for M06-2x (2.74 kcal/mol) only differs by 0.34 kcal/mol from the MP2 average one (2.40 kcal/mol). The other functionals tested also provide reasonable values, with average values close to the MP2 ones, 2.85 and 2.92 kcal/mol for B3LYP-D3 and WB97XD, respectively. The B3LYP average relative energy is the one with the largest variation with respect to the MP2 values, being 0.92 kcal/mol larger. In Fig. 3a the overlap between the different structures of **6np** calculated at all the levels is shown. As observed, their structural changes are minor across the different methods showing RMSD with respect to the MP2 structure of 0.128 (B3LYP), 0.053 (B3LYP-D3), 0.041 (W97XD) and 0.043 (M06-2x) Å. Despite all the structures being very similar, the RMSD of B3LYP is more than twice that of any other one.

So, for all further calculations, only the M06-2x functional results were used (see Table S1 for Cartesian Coordinates), allowing for the study of larger systems, where the MP2 calculations would be very computationally demanding, thus giving a good accuracy compromise. The B3LYP results are also shown, in certain cases, for comparison with the existing data in the literature, which use this functional.

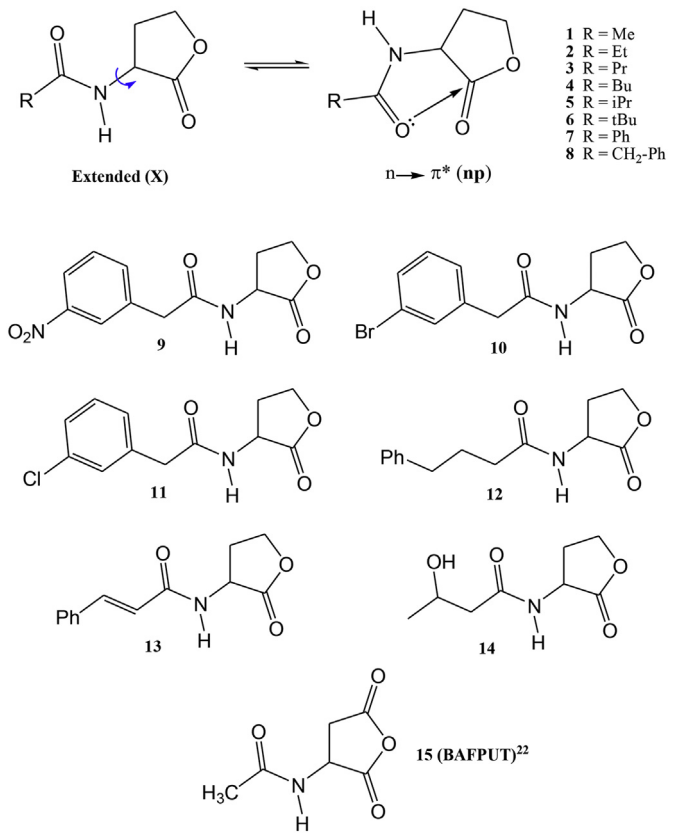

Fig. 2. Compounds included in this study. The extended conformation is denoted **X**, while **np** indicates the conformation with an n → π* interaction.

Table 1
Relative energies (in kcal/mol) obtained as the difference between the **X** and **np** conformations. Positive values indicate that extended conformation **X** is more stable. All the calculations done in gas phase at the DFT/6-311 + G(2d,p) computational level and at the MP2/6-311 + G(2d,p) level.

Compound	B3LYP	B3LYP-D3	M06-2x	WB97XD	MP2
1	3.35	2.91	2.81	2.70	2.48
2	3.13	2.74	2.63	2.70	2.28
3	3.23	2.76	2.54	3.02	2.34
4	3.22	2.76	2.37	2.78	2.37
5	3.23	2.63	2.44	2.80	2.14
6	3.24	2.73	2.72	2.75	2.23
7	3.87	3.44	3.66	3.71	2.98

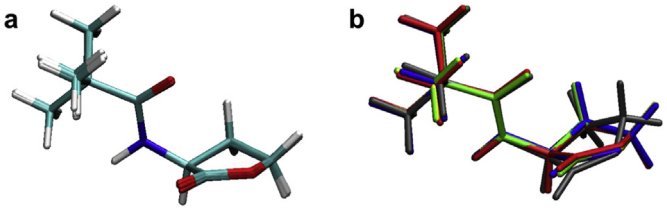

Fig. 3. a) Overlap between the **np** conformations of **6** at MP2, B3LYP, B3LYP-D3, M06-2x and WB97XD levels. b) Overlap between **np** conformations of 6 (from reference [14] (in grey)) in gas phase and calculated in the present work in gas phase (blue), chloroform (red), acetonitrile (yellow) and water (green) solvent models. (For interpretation of the references to colour in this figure legend, the reader is referred to the web version of this article.)

Table 2
Relative energies (in kcal/mol) obtained as the difference between the energies for the **X** and **np** conformations. Positive values indicate that the **X** conformation is more stable while negative values show that **np** conformation is more stable.

	B3LYP				M06-2×			
	gas	$CHCl_3$	CH_3CN	H_2O	gas	$CHCl_3$	CH_3CN	H_2O
1	3.35	1.72	0.90	0.85	2.81	0.83	−0.40	−0.55
2	3.13	1.59	0.96	0.94	2.63	0.67	−0.46	−0.59
3	3.23	1.65	1.02	0.94	2.54	0.86	−0.39	−0.38
4	3.22	1.87	0.99	0.91	2.37	0.82	−0.33	−0.46
5	3.23	1.75	0.92	0.84	2.44	0.63	−0.53	−0.22
6	3.24	1.72	0.94	0.89	2.72	0.79	−0.45	−0.58
7	3.87	1.94	0.84	0.73	3.66	1.17	−0.16	−0.31
8	3.27	1.62	0.88	0.85	0.80	1.00	−0.35	−0.45
9	4.04	2.10	0.93	0.84	3.38	0.76	−0.44	−0.47
10	3.47	1.67	0.82	0.71	2.66	0.44	−0.25	−0.36
11	3.43	1.75	0.90	0.86	2.70	0.95	−0.29	−0.64
12	3.21	1.67	0.87	0.84	2.33	0.36	−0.33	−0.51
13	3.54	1.88	0.92	0.89	2.89	0.74	−0.54	−0.68
14	3.43	1.69	1.03	0.95	2.89	1.05	−0.09	−0.22
15	1.22	−0.22	−0.50	−0.68	0.19	−1.66	−2.72	−2.83

It was previously found for the OHLs that inclusion of the solvent effect has a direct impact on the relative stability of the corresponding **X** and **np** conformations [5]. Therefore, the calculations were extended to include a different solvent, using the PCM model for the B3LYP and M06-2x functionals, to see if the solvent effect was similar to that observed for the OHLs. The range of compounds studied (**1–15**) was also increased to include biologically active non-natural AHL analogues (**8–13**), and compound **14** to study the effect of a HB donor in the alkyl chain. The final compound (**15**) was included as it has a published x-ray crystal structure in the Cambridge Structural Database (denoted as BAFPUT). [22] It is not an AHL but has the lactone head group replaced with a succinic anhydride moiety, which contains an extra carbonyl group.

As can be seen in Table 2, inclusion of the solvent model has a significant impact on the relative energy differences of the **X** and **np** conformations for all the compounds studied. In all cases, the gas phase calculations show that the extended conformation (**X**) is more stable than the conformation showing an n → π* interaction (**np**). This is true for both the B3LYP and M06-2x functional values. When the solvent is taken into account (chloroform) there is a significant reduction in the relative stabilities but still favouring the extended (**X**) conformation. Increasing the polarity of the solvent (acetonitrile and water) reduces the relative energy difference between the **X** and **np** conformations. Importantly, when the M06-2x functional is used, with acetonitrile as solvent, there is a switch in the relative stability, i.e., the **np** conformation becomes more stable. Excluding compound **15**, the average relative energies found were 3.41, 1.76, 0.92, and 0.86 kcal/mol with B3LYP (GP, $CHCl_3$, CH_3CN and H_2O, respectively) and 2.63, 0.79, −0.36, and −0.48 kcal/mol with the M06-2x functional. The use of a functional such as M06-2x decreases the relative energy ~1 kcal/mol, and this is particularly important when dealing with very weak interactions. Furthermore, the Bolztmann distributions of the **X** conformer for each AHL compound (**1–14**) across the range of solvents are shown in Table S2. Following the energy pattern, the **X** conformation is the major conformer when using B3LYP regardless of the solvent being studied. However, when the M06-2x results are taken into account, the percentage of the **np** conformation becomes slightly more dominant, particularly in the more polar solvents. In Fig. 3b, the overlap between the calculated structure (from reference[14]) in the gas phase (grey) and the one calculated at the M06-2x in the gas phase (blue), chloroform (red), acetonitrile (yellow) and water (green) is shown. As observed, some structural differences are observed with respect to the compound from reference [14] showing a RMSD of 0.851 (gas phase), 0.865 (chloroform), 0.860 (acetonitrile) and 0.860 (water) Å.

This raises two main issues, firstly, the necessity to use a functional with long range dispersions included, and secondly, the importance of solvent effects on the relative energy differences for the two conformations.

Previously we have studied the relative energies for the corresponding OHLs containing the extra 3-oxo group in the alkyl chain [5]. In particular, the relative energy differences between the corresponding extended conformation (compound **A** in ref. [5]) and the one showing n → π* interactions (compound **B** in ref. [5]) were found to be 0.63, 0.63, 0.61 and − 0.17 kcal/mol for the gas phase, chloroform, acetonitrile and water, respectively, using B3LYP/6–311 + +G(d,p) [5]. The results in Table 2 show that although the relative stability of the OHL conformations was dependent on the solvent used, for the AHLs this effect is significantly more evident, i.e. the evolution of the relative energy across the solvent is more pronounced in AHLs than in OHLs, considering the same functional (B3LYP), but also if a different functional, such as M06-2x, is used.

In order to provide further insight into the conformations of the AHLs, the intramolecular O···C ($d_{O\cdots C}$) distance and different dihedral angles, D_1 and D_2 (Fig. 4), have been analysed and their values are summarised in Table 3 and Table S2. The $d_{O\cdots C}$ distance was defined as the distance between the oxygen of the amide carbonyl and the carbon of the lactone carbonyl.

As observed, the **np** structures present shorter values of the $d_{O\cdots C}$ than the **X** structures due to the interaction between both carbonyl groups. In the case of the **np** structures the $d_{O\cdots C}$ intramolecular distances are shorter than the sum of their respective van der Waals radii (1.70 + 1.52 = 3.22 Å) [23]. The shortest distance is found for compound **15** (2.731 Å in the gas phase) which is significantly shorter than the rest of AHLs, followed by **5** (R = ^{t}Bu). The $d_{O\cdots C}$ distance also evolves with the solvent model used, being shorter in polar solvents such as acetonitrile and water, than in chloroform and in the gas phase. This observed shortening of the $d_{O\cdots C}$ distance, across the solvent range studied can be up to 0.053 Å, when comparing the gas phase data with the data for water. Again, the influence of the solvent on the n → π* interaction is clearly evident. However, within the extended structure, the solvent effects are less pronounced. This was expected since no n → π* interaction is found in the **X** conformations.

The degree of planarity of each conformation was evaluated using the dihedral angles D_1 and D_2 (Fig. 4). D_1 is defined by both carbonyl groups (O=C…C=O) and D_2 is defined by N−H of the amide and the carbonyl group in the lactone. It was found that for all **np** conformations for compounds **1–15** (Table 3), D_1 shows narrower values than in

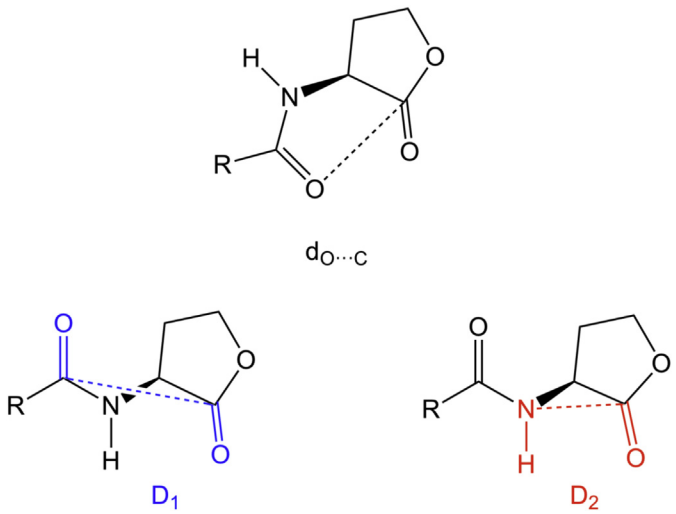

Fig. 4. Distance $d_{O\cdots C}$ and dihedral angles (D_1 and D_2) analysed for the **X** and **np** conformations, for compounds **1–15.**

Table 3
Intramolecular O···C distances, in Å, and dihedral D1 and D2 angles, in °, of compounds **1–15**, at the M06-2x/6–311 + G(2d,p) computational level, in gas phase and PCM solvent models.

	np				X			
	GP	$CHCl_3$	CH_3CN	H_2O	GP	$CHCl_3$	CH_3CN	H_2O
					$d_{O\cdots C}$			
1	2.816	2.797	2.783	2.781	4.203	4.209	4.210	4.210
2	2.831	2.801	2.794	2.793	4.204	4.211	4.211	4.211
3	2.832	2.801	2.788	2.781	4.203	4.209	4.207	4.207
4	2.831	2.796	2.781	2.781	4.204	4.210	4.207	4.207
5	2.811	2.793	2.780	2.778	4.203	4.213	4.210	4.211
6	2.788	2.769	2.758	2.757	4.184	4.190	4.189	4.189
7	2.830	2.790	2.780	2.779	4.186	4.195	4.200	4.200
8	2.828	2.798	2.787	2.786	4.213	4.220	4.214	4.213
9	2.830	2.792	2.785	2.792	4.211	4.221	4.206	4.221
10	2.824	2.794	2.792	2.792	4.214	4.211	4.217	4.216
11	2.808	2.787	2.780	2.780	4.212	4.221	4.213	4.220
12	2.835	2.790	2.783	2.782	4.204	4.210	4.213	4.213
13	2.807	2.795	2.783	2.783	4.204	4.213	4.216	4.216
14	2.821	2.794	2.786	2.785	4.204	4.208	4.211	4.211
15	2.731	2.690	2.675	2.674	4.873	4.878	4.876	4.875
					D1			
1	103.6	98.7	95.4	95.3	−156.1	−152.9	−149.8	−149.6
2	104.0	98.6	96.3	96.0	−156.2	−153.5	−150.5	−150.3
3	103.9	98.6	96.2	95.6	−155.9	−152.9	−150.5	−150.3
4	103.9	98.6	96.2	95.4	−155.9	−154.4	−150.5	−150.3
5	104.6	99.0	96.4	96.2	−156.4	−154.1	−149.4	−149.2
6	104.0	99.3	96.3	96.1	−155.7	−153.0	−149.7	−149.5
7	102.6	97.4	95.5	95.3	−154.6	−152.3	−150.7	−150.4
8	103.8	98.4	95.7	95.5	−158.3	−155.8	−150.0	−149.4
9	103.7	98.1	95.8	95.5	−155.2	−154.1	−148.8	−151.9
10	102.5	98.5	95.8	95.6	−155.1	−153.2	−151.6	−151.0
11	101.8	97.3	96.0	95.8	−155.5	−152.5	−150.8	−151.0
12	103.4	99.0	95.6	95.4	−157.2	−154.1	−151.7	−151.4
13	103.5	98.0	95.4	95.2	−157.1	−153.9	−151.4	−151.0
14	103.0	98.4	96.0	95.8	−155.8	−151.7	−149.8	−149.5
15	107.7	104.5	103.0	102.9	−155.7	−152.4	−149.4	−149.0
					D2			
1	−53.1	−63.4	−70.6	−70.8	11.6	17.6	22.9	23.1
2	−52.6	−62.6	−68.9	−69.7	11.0	16.3	21.4	21.6
3	−52.8	−63.4	−69.6	−70.7	10.8	16.2	21.7	21.9
4	−53.0	−63.4	−69.3	−70.9	10.9	16.2	21.4	21.6
5	−52.6	−62.7	−68.5	−68.9	11.9	16.8	23.6	23.8
6	−54.2	−64.0	−69.8	−70.4	12.3	17.5	23.0	23.3
7	−63.5	−76.3	−80.2	−80.6	6.2	10.9	14.2	14.7
8	−52.3	−63.7	−70.0	−70.5	6.7	13.8	22.2	23.2
9	−53.7	−63.9	−70.0	−71.0	13.9	16.8	23.0	19.9
10	−56.3	−63.5	−70.0	−70.6	14.3	16.0	20.3	21.4
11	−55.8	−65.6	−69.6	−70.1	13.6	18.8	21.4	21.7
12	−53.4	−62.4	−70.5	−71.0	11.0	16.6	20.8	21.4
13	−51.8	−63.3	−70.0	−70.5	9.7	15.8	20.7	21.3
14	−55.7	−64.6	−70.2	−70.7	13.0	19.0	22.9	23.4
15	−47.8	−56.0	−60.6	−61.0	10.8	17.2	23.0	23.8

the **X** conformations, fully consistent with the n → π* interactions in the former. As occurred with the intramolecular $d_{O\cdots C}$ distances, D_1 becomes more narrow with the polarity of solvent model used, i.e., the larger dielectric constant, the narrower D_1. Again, this is consistent with the relative energies and $d_{O\cdots C}$ distance values found. The **X** conformations also present narrower D_1 angles in water and acetonitrile than in the gas phase and chloroform. For all media studied the D1 dihedral is within the range observed for n → π* interactions in the literature and are close to the Burgi-Dunitz angle.

It was found that the D_2 dihedral angle becomes wider with the solvent polarity, both in the **np** and **X** conformations, but the observed changes in moving from the gas phase to water are more pronounced in the **np** conformations, in which the N—H group becomes systematically less coplanar with the lactone carbonyl.

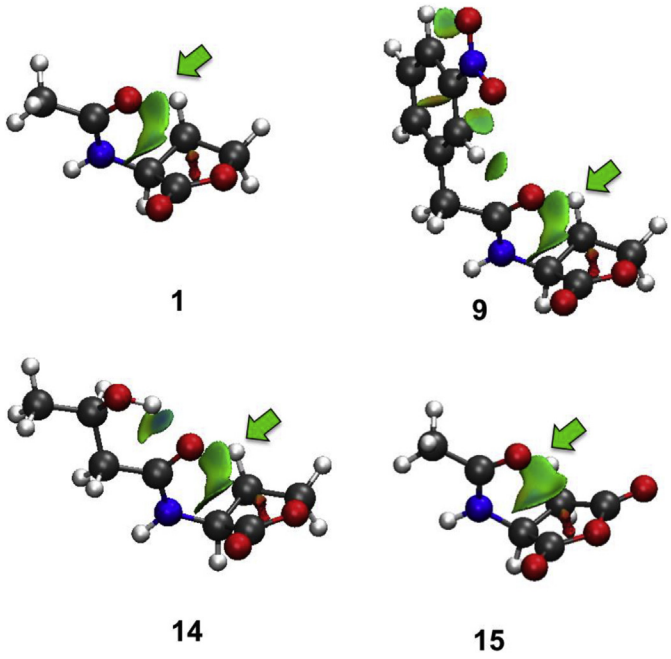

Fig. 5. Non-covalent interaction (NCI) plots for the **np** conformations of **1, 9, 14** and **15**, in acetonitrile. Green areas correspond to $\lambda_2 \approx 0$ (weak). λ_2 is one of the three eigenvalues of the electron density Hessian with $\lambda_1 \leq \lambda_2 \leq \lambda_3$ [12]. (For interpretation of the references to colour in this figure legend, the reader is referred to the web version of this article.)

3.3. Electron density properties

We have carried out Atoms in Molecules (AIM) analysis in order to evaluate the possible bond critical points (BCP), particularly for the **np** conformations. Molecular graphs of all the compounds studied can be found in Fig. S1. Unfortunately, as occurred for the OHLs, no BCPs were found associated with the interaction between the amide group oxygen atom and the C═O atoms of the carbonyl of the lactone. However, as is known from the literature, the absence of BCPs does not imply the absence of interaction [24–25].

We have taken advantage of the Non-Covalent Indices (NCI) plots to qualitatively evaluate the possible interactions in the **np** conformations. In Fig. 5 NCI plots are depicted, in which the green areas shown correspond to regions of weak interactions associated with values of $\lambda_2 \approx 0$, where λ_2 is one of the three eigenvalues of the electron density Hessian [12]. Those green areas (marked with a green arrow) indicate that there is an interaction between the amide oxygen, acting as electron donor, and the lactone carbonyl, as electron acceptor. Similar plots were found in the case of the OHLs [5]. As previously observed, the n → π* donation was reported by Raines [14–16], being reminiscent of the Bürgi–Dunitz trajectory for nucleophilic additions to carbonyl groups which can cause pyramidalisation of the acceptor carbonyl group [26–28]. However, as mentioned this is a precursor of the nucleophilic addition but since the n → π* donation is very weak, no sign of pyramidalisation was observed.

It is also worth noting that compound **14**, which contains an O—H group in the alkyl side-chain, presents an intramolecular HB (IMHB). The H···O distance is 1.972 Å, with an electron density on the bond critical point (ρ_{BCP}) of 0.0253 a.u. and a Laplacian value, $\nabla^2\rho_{BCP}$, of 0.0989 a.u. These are in the same range as those found for other HBs reported in the literature. This interaction contributes to the planarity of the molecule increasing the linearity of the carbon backbone.

3.4. Natural bond order analysis

Natural bond orbital (NBO) theory was utilised to evaluate the

Table 4
Second order orbital interaction energies, E(2) (in kcal/mol) corresponding to the donation from the amide oxygen lone pair into the lactone π* C═O antibonding orbital.

	GP	$CHCl_3$	CH_3CN	H_2O
1	1.30	1.61	1.80	1.81
2	1.15	1.53	1.66	1.68
3	1.15	1.55	1.73	1.80
4	1.17	1.60	1.76	1.81
5	1.20	1.54	1.73	1.74
6	1.39	1.70	1.91	1.92
7	1.26	1.65	1.75	1.76
8	1.15	1.55	1.71	1.72
9	1.13	1.54	1.66	1.65
10	1.30	1.54	1.66	1.66
11	1.39	1.69	1.72	1.73
12	1.14	1.59	1.75	1.76
13	1.37	1.62	1.76	1.76
14	1.12	1.39	1.49	1.50
15	2.06	2.80	3.09	3.12

charge transfer in terms of orbital interactions between the electron lone pairs of the amide oxygen into the lactone carbonyl π* antibonding orbital. The second order orbital interaction energies, E(2) in kcal/mol, are summarised in Table 4. As can be seen, the E(2) values range from 1.12 to 2.06 kcal/mol in the gas phase. Significantly, when solvent models are included there is an increase in the orbital interaction energies, which gradually increase with the polarity of the solvent, being maxima in the water solvent model. These correlate with the observed shortening of the $d_{O\cdots C}$ distances for the **np** conformations, as seen in Table 3. Overall, the AHLs show larger E(2) values than those found for the OHLs, in which the E(2) values were found to be 1.01 kcal/mol and 1.02 kcal/mol for the acetonitrile and water models, respectively [5]. This not only confirms the existence of the $n \rightarrow \pi^*$ donation but also the important influence of the solvent on this interaction. Finally, it is worth noting that compound **15** (crystal structure BAFPUT) [22] presents the largest donation, being almost twice as large (~3 kcal/mol) as all the compounds studied across the different solvents. This is most likely because of the presence of the second electron-withdrawing carbonyl group in the lactone ring.

4. Conclusions

We have carried out a computational study on a total of 14 different AHLs and one crystal structure AHL-like compound (BAFPUT)[22] with attention to the relative stability between the extended conformation **X** and the **np**, i.e. that conformation showing a $n \rightarrow \pi^*$ interaction between the amide carbonyl and lactone carbonyl.

The benchmark performed suggested that functionals including long range dispersion, such as M06-2x are more convenient to describe weak interactions rather than the B3LYP functional. Solvent effects were analysed to evaluate the variation of the relative energy between both conformers with the dielectric constant of the solvent. It was found that **np** conformers are more favoured when polar solvents are taken into account. Importantly, this indicates that $n \rightarrow \pi^*$ interactions become stronger with the polarity of the solvent used. That fact was not only observed by the increase on the relative energy in favour to the **np** conformer, but also in the decrease of the O···C distances and the second order orbital interaction energies.

Finally, when a comparison between OHLs and AHLs is done, it was found that AHLs present **np** conformers that are more stabilised than for the OHLs, with shorter O···C distances, larger relative energies and larger E(2) in AHLs, with respect to OHLs.

Conflict of interest

There are no conflicts of interest to declare.

Acknowledgements

We are grateful to the Higher Education Authority's (PRTLI IV) Programme for Research in Third-Level Institutions (Cycle IV) for funding for AN, and to the Irish Research Council (GOIPG-2013-379) and VEC Dublin for funding for DC. Thanks are given to the Irish Centre for High-End Computing (ICHEC) for the provision of computational facilities.

Appendix A. Supplementary data

Supplementary data to this article can be found online at https://doi.org/10.1016/j.bpc.2018.04.002.

References

[1] World Health Organisation, Antimicrobial Resistance: Global report on surveillance, http://www.who.int/drugresistance/documents/surveillancereport/en/, (**2014**) (Accessed on March 7th 2018).
[2] S. Atkinson, P. Williams, Quorum sensing and social networking in the microbial world, J. R. Soc. Interface 6 (2009) 959.
[3] M. Schuster, D. Joseph Sexton, S.P. Diggle, E. Peter Greenberg, Acyl-homoserine lactone quorum sensing: from evolution to application, Annu. Rev. Microbiol. 67 (2013) 43–63.
[4] V.C. Kalia, Quorum sensing inhibitors: an overview, Biotechnol. Adv. 31 (2013) 224–245.
[5] D. Crowe, A. Nicholson, A. Fleming, E. Carey, G. Sánchez-Sanz, F. Kelleher, Conformational studies of Gram-negative bacterial quorum sensing 3-oxo N-acyl homoserine lactone molecules, Bioorg. Med. Chem. 25 (2017) 4285–4296.
[6] Y. Zhao, D. Truhlar, The M06 suite of density functionals for main group thermochemistry, thermochemical kinetics, noncovalent interactions, excited states, and transition elements: two new functionals and systematic testing of four M06-class functionals and 12 other functionals, Theor. Chem. Accounts 120 (2008) 215–241.
[7] M.J. Frisch, J.A. Pople, J.S. Binkley, Self-consistent molecular-orbital methods .25. Supplementary functions for Gaussian-basis sets, J. Chem. Phys. 80 (1984) 3265–3269.
[8] R.F.W. Bader, Atoms in Molecules: A Quantum Theory, Clarendon Press, Oxford, 1990.
[9] Keith, T. A. Aimall, Tk Gristmill Software (Aim.Tkgristmill.Com), 16.01.09; 2011.
[10] A.E. Reed, L.A. Curtiss, F. Weinhold, Intermolecular interactions from a natural bond orbital, Donor-Acceptor Viewpoint, Chem. Rev. 88 (1988) 899–926.
[11] E.D. Glendening, C.R. Landis, F. Weinhold, Nbo 6.0: natural bond orbital analysis program, J. Comput. Chem. 34 (2013) 1429–1437.
[12] E.R. Johnson, S. Keinan, P. Mori-Sanchez, J. Contreras-Garcia, A.J. Cohen, W. Yang, Revealing noncovalent interactions, J. Am. Chem. Soc. 132 (2010) 6498–6506.
[13] W. Humphrey, A. Dalke, K. Schulten, Vmd: visual molecular dynamics, J. Mol. Graph. 14 (1996) 33–38.
[14] R.W. Newberry, R.T. Raines, A key n→π* interaction in *N*-acyl homoserine lactones, ACS Chem. Biol. 9 (2014) 880–883.
[15] A. Choudhary, R.W. Newberry, R.T. Raines, n→π* interactions engender chirality in carbonyl groups, Org. Lett. 16 (2014) 3421–3423.
[16] R.W. Newberry, B. VanVeller, I.A. Guzei, R.T. Raines, N→π* interactions of amides and thioamides: implications for protein stability, J. Am. Chem. Soc. 135 (2013) 7843–7846.
[17] A.D. Becke, Density-Functional Thermochemistry .3. The Role of Exact Exchange, J. Chem. Phys. 98 (1993) 5648–5652.
[18] C.T. Lee, W.T. Yang, R.G. Parr, Development of the Colle-Salvetti correlation-energy formula into a functional of the electron-density, Phys. Rev. B 37 (1988) 785–789.
[19] S. Grimme, J. Antony, S. Ehrlich, H. Krieg, A consistent and accurate ab initio parametrization of density functional dispersion correction (Dft-D) for the 94 elements H-Pu, J. Chem. Phys. 132 (2010) 154104.
[20] J.-D. Chai, M. Head-Gordon, Long-range corrected hybrid density Functionals with damped atom-atom dispersion corrections, Phys. Chem. Chem. Phys. 10 (2008) 6615–6620.
[21] C. Møller, M.S. Plesset, Note on an approximation treatment for many-electron systems, Phys. Rev. 46 (1934) 618–622.
[22] C.R. Groom, I.J. Bruno, M.P. Lightfoot, S.C. Ward, The Cambridge structural database, Acta Crystallogr. Sect. B 72 (2016) 171–179.
[23] A. Bondi, Van Der Waals volumes and radii, J. Phys. Chem. 68 (1964) 441–451.
[24] J. Poater, M. Solà, F.M. Bickelhaupt, A model of the chemical bond must be rooted in quantum mechanics, provide insight, and possess predictive power, Chem. Eur. J. 12 (2006) 2902–2905.
[25] J. Poater, M. Solà, F.M. Bickelhaupt, Hydrogen–hydrogen bonding in planar biphenyl, predicted by atoms-in-molecules theory, Does Not Exist, Chem. Eur. J. 12 (2006) 2889–2895.
[26] L.M. Azofra, S. Scheiner, Tetrel, Chalcogen, and Ch·O hydrogen bonds in complexes pairing carbonyl-containing molecules with 1, 2, and 3 molecules of Co_2, J. Chem. Phys. 142 (2015) 034307.
[27] M. Altarsha, F. Ingrosso, M.F. Ruiz-Lopez, A new glimpse into the Co_2-philicity of carbonyl compounds, ChemPhysChem 13 (2012) 3397–3403.
[28] E. San-Fabián, F. Ingrosso, A. Lambert, M.I. Bernal-Uruchurtu, M.F. Ruiz-López, Theoretical insights on electron donor–acceptor interactions involving carbon dioxide, Chem. Phys. Lett. 601 (2014) 98–102.